

Structure and metastability of superheated Al(111)

G. Bilalbegović

Fakultät für Physik, Universität Bielefeld, D-33615 Bielefeld, Germany

(February 1, 2008)

The high-temperature properties of the Al(111) surface are studied by molecular-dynamics simulation. This surface does not melt below the bulk melting point, but can be superheated. Superheating of metal surfaces has been recently observed in several experiments. A molecular-dynamics study of the structural properties reveals how after going through the superheating regime melting occurs over the whole crystal in a narrow temperature range. The temperature dependence of the surface stress, the mean-square vibrational amplitudes and the anomalous outward expansion of the distance between two top layers are calculated. A transition from superheated to liquid state is analyzed using kinetic description for the formation of liquid nuclei by the Fokker-Planck equation and conservation of heat at the liquid-solid interface.

68.35.Rh,64.60.My,64.70.Dv

I. INTRODUCTION

The question of how melting occurs, in spite of its long history and importance, remains to a large extent unanswered. Although various metastable phases of different materials are present in nature, for some time it was a common belief that metastability is not possible at the solid-to-liquid transition. The argument was that a free surface of any material in contact with vapor acts as a nucleus of a liquid phase and suppresses superheating, i.e., nonmelting above the bulk melting temperature. Nevertheless, superheating was recently observed in several materials. For metal crystals it is especially difficult to achieve superheating. The viscosity of liquid metals is low and the liquid-solid interface rapidly propagates into the bulk. Several ways to suppress melting of metals were found. One way was to enclose the metal crystal into another metal with higher melting temperature. For example, superheating up to 62 K was observed for small Pb precipitates in Al¹. It was checked that the Pb particles of mean size $\sim 200 \text{ \AA}$ remain superheated at 18 K above the bulk melting point for more than 21 hours¹. The Ag spheres were coated with Au and superheated by 25 K for a period of about one minute². Such a behavior was modeled in molecular-dynamics (MD) simulation using the Lennard-Jones potentials and different strength of interaction³.

Techniques to superheat clean metal surfaces were also developed. It is known that at the temperatures below the bulk melting point some metal surfaces exhibit surface melting. Using medium-energy ion scattering it was found that the Pb(110) surface melts and that the thickness of liquid layer diverges when the temperature approaches the bulk melting point⁴. On the contrary, Pb(111) does not melt and Pb(100) exhibits incomplete melting characterized by the presence of liquid diffusion only in one or two topmost layers⁴. Similar behavior show low-index surfaces of other fcc metals, in particular surfaces of aluminum⁵. It was also found that some close-packed metal surfaces under special conditions may exhibit superheating. Herman and coworkers have found superheating by 120 K for Pb(111)⁶, 90 K for Bi(0001)⁷, and even 15 K for incompletely melted Pb(100)⁸. Superheating of these surfaces was studied by time-resolved reflection high-energy electron diffraction. Melting was prevented by rapid heating with a pulsed laser beam. Using laser pulses of the width $\sim 10^2 \text{ ps}$ it was possible to bypass melting by inducing large heating and cooling rates of about 10^{11} K/s . By applying the same procedure it was not possible to superheat the Pb(110) surface^{9,10}. Superheating was also found in MD simulation of laser-pulse irradiation for Cu(111)¹¹. For a development of new methods in materials processing by the laser beams it is important to understand the properties of superheated surfaces.

Small crystallites bounded by nonmelting facets show superheating. For example, nonequilibrium octahedral lead crystallites on graphite (made up of the (111) facets and small round parts) exhibit superheating by several K and for several hours¹². Similar superheating was also observed in MD high-temperature studies for Au(111)¹³, Al(111)¹⁴, Cu(111)¹⁵, and Pb(111)¹⁶. DiTolla and coworkers have performed MD simulation for deposition of a liquid aluminum cluster on the melting Al(110) and nonmelting Al(111) surfaces¹⁴. They used these results and thermodynamic arguments to connect superheating with the wetting angle and the non-melting induced faceting angle¹⁶. The type of superheating related to fcc(111) is enabled by the exclusive presence of these non-melted surfaces on the specially prepared crystallites and on MD slabs. On equilibrium crystals the surface-melted facets (such as fcc(110)) are also present. They act as a nucleus of the liquid phase and prevent superheating of the whole crystal.

Till now the studies of superheating phenomena have been mainly concentrated on the means to achieve the superheated state. In this work MD simulation method was used to study the properties of this metastable state, in particular the superheated Al(111) surface. The analysis of the mean-square displacements, surface relaxation, MD particle trajectories, and surface stress has been carried out. The results of kinetic theory based on the Fokker-Planck equation¹⁷ and an analysis of the heat transport at the liquid-solid interface^{18,19} were used to estimate the maximum superheating temperature for aluminum. This analysis employed several quantities that were experimentally determined and deduced from MD simulations. In the following the MD simulation method is described in Sec. II. Results of simulation and discussion are presented in Subsec. III A. Subsection III B deals with the kinetic analysis of transition from the superheated to liquid state. A summary and conclusions are given in Sec. IV.

II. MOLECULAR-DYNAMICS COMPUTATIONS

The structure of the aluminum surface at high temperatures was studied by MD simulation. The interatomic interactions were derived from a classical many-body potential²⁰. This form of potentials gives a proper physical picture of metallic bonding²¹. The optimal set of parameters in the potential was found by the force-matching fitting to *ab initio* electronic structure calculations using a numerical optimization procedure²⁰. The data used for fitting were generated from different geometries, both at $T = 0$ K and for finite temperatures. As a result the potential is characterized by a good transferability. This potential was already used in MD simulations and it reproduced well experimental results for bulk and surface properties of aluminum^{14,20,22}. The melting point $T_m = 939 \pm 5$ K is in good agreement with the experimental value of 933.52 K²³. The calculated bulk melting temperature was precisely determined by simulating coexisting liquid and solid phases under constant energy^{24,25}.

The simulation of the high-temperature properties of the Al(111) surface started at $T = 0$ K. The MD box of 1600 particles was used. These atoms were arranged in the usual single slab geometry with the thickness of $N_z = 16$ (111) layers (i.e., $\sim 35\text{\AA}$), and a 10×10 square lattice in each layer. As in other classical MD studies of surfaces, the slab was extended along x and y by using periodic boundary conditions and no boundary conditions were used along z . The three bottom layers of the slab were kept fixed to simulate the bulk. The lattice constant was changed with temperature according to the expansion coefficient found in MD simulation under zero pressure. The time step of 2.64×10^{-15} s was used. Most runs were carried out at the constant temperature (i.e., in the canonical ensemble). The temperature was controlled by rescaling the particle velocities at each time step. At each temperature at least 10^4 time steps were performed to ensure thermal equilibration. In the superheating regime the length of the runs was much longer, i.e., up to 10^6 time steps. In this regime simulations at fixed energy were also performed and the same results as in the canonical ensemble were obtained.

The stress analysis often shows important changes of surface properties. The surface stress tensor σ_{ij} is given by

$$\sigma_{ij} = \gamma\delta_{ij} + \frac{\partial\gamma}{\partial\epsilon_{ij}}, \quad (1)$$

where γ is the surface free energy per unit area, δ_{ij} is the Kronecker symbol, ϵ_{ij} is the surface strain tensor, and i, j are directions in the surface plane²⁶. The surface stress can be obtained from the components of the pressure tensor calculated during MD simulation²⁷. In the computation of the stress MD boxes equilibrated for at least 10^5 time steps were used.

III. RESULTS AND DISCUSSION

A. Structure

The studies of the various structural properties of the Al(111) surface (such as the density, the static structure factor, the orientational order parameter, and MD particle trajectories) were done. The detailed analysis of these properties between 0 K and 1500 K shows that at ~ 1120 K melting starts on a typical MD simulation time scale. The temperature of 1050 K was selected for a detailed analysis of the superheating regime. At this temperature the surface stays superheated after 10^6 time steps. The static structure factor, the density and order parameter plots (not presented here), as well as the MD particle trajectories in Fig. 1 show that the superheated Al(111) surface at 1050 K and after 10^6 time steps is crystalline and well ordered. It was found that in the superheating regime single adatoms often appear above the surface (see Fig. 1 (b)). These adatoms have a very short life time ($\sim 10^{-12}$ s). This is in contrast with the results obtained using the same type of potentials for the high-temperature behavior of

fcc(110) (surface melting)²⁸ and fcc(100) (incomplete melting)²⁹. For these surfaces the formation of adatoms was not observed. The Al(111) surface at $T=1120$ K stays superheated for a long time of 4×10^5 MD steps. In the interval of $(40 - 45) \times 10^4$ time steps melting begins and develops. It was found that at this temperature melting proceeds with different speed in different MD runs. For example, while in one run eleven layers were melted after 42×10^4 MD steps, in another one after 45×10^4 time steps only five top layers of MD box were melted. Internal energy as a function of temperature is shown in Fig. 2. The jump region on the caloric curve between the crystalline and liquid states is less abrupt than usually for melting transitions. The maximum superheating temperature estimated in this simulation is 180 K. DiTolla and coworkers reported ~ 150 K for the same surface, using the same potential and similar simulation times¹⁴. This is a result of different shape and size of MD boxes used in these simulations. A dependence of the calculated bulk melting temperature on the size, shape, and orientation of the samples is well known problem in MD simulation^{24,25}.

The surface stress was calculated and its temperature dependence is presented in Fig. 3. The (111) surface is isotropic, the xx and yy components of the stress tensor are approximately equal and therefore the stress is represented by their mean values. The stress of 0.056 eV \AA^{-2} was found for the relaxed surface at $T = 0$ K. This is 3.3 times less than the average stress for Au(110) at the same temperature and for the same type of potential³⁰. The calculated stress for Al(111) at $T = 0$ K is in excellent agreement with 0.059 eV \AA^{-2} obtained for the same surface in MD simulation using the Sutton-Chen potential³¹. These MD results should be compared with two *ab initio* electronic structure calculations for Al(111). The value of 0.078 eV \AA^{-2} was found by Needs and Godfrey³² and 0.090 eV \AA^{-2} by Feibelman³³. Schmid and coworkers calculated surface stress for some low-index fcc metal surfaces using MD simulation and effective medium theory potentials³⁴. They found that MD generally gives lower values compared to electronic structure calculations. Figure 3 shows that surface stress for Al(111) is almost constant between $T = 0$ K and $T = 900$ K. The stress is always tensile. The components of any type of stress (or pressure) tensor calculated in MD simulation exhibit large fluctuations³⁵. In Fig. 3 the errors increase with the temperature and the maximum of statistical uncertainty for the points is 20%. Same trend in the distribution of the values (i.e., that the stress remains almost constant over the wide temperature region and also that pronounced scatter of the data exists) was found in MD simulation for the (111) surface of the Lennard-Jones crystal²⁷. It is well known that surface stress [see Eq. (1)] for a liquid becomes equal to the surface free energy (i.e., $\partial\gamma/\partial\epsilon_{ij} = 0$). The value 0.05 eV \AA^{-2} , obtained in this simulation for the liquid surface at $T = 1500$ K, is equal to the surface free energy of liquid aluminum⁴.

The mean-square vibrational amplitudes for the surface atoms are shown in Table I. The values of mean-square displacements are presented at two temperatures below the bulk melting point (300 K and 900 K) and also at 1050 K, i.e., for a typical temperature in the superheating region. The last row of this table is obtained for the solid surface at the onset of melting at $T = 1120$ K. The values found for temperatures below the bulk melting point are in a good agreement with other MD simulation results^{29,36,37}. The mean-square vibrational amplitudes at the end of the superheating region (not studied elsewhere) are ~ 10 times larger than below the bulk melting temperature. The mean-square amplitudes of vibration are isotropic at all temperatures. Most MD simulations of the high-temperature properties of fcc metal surfaces also show that the mean-square vibrational amplitudes are isotropic^{36,37}. In recent experimental studies³⁸ and MD simulation²⁹ of two fcc(100) surfaces it was found that the mean-square amplitudes of vibration are anisotropic. Out-of-plane vibrational amplitudes were found to be smaller than in-plane ones. This reveals lateral disordering typical for incomplete melting. Isotropic mean-square vibrational amplitudes found here for Al(111) show that after superheating regime melting proceeds in similar way along all directions.

Most low-index metal surfaces relax inwards at lower temperatures. It is known that the Al(111) surface exhibits an anomaly in relaxation, i.e., that at low temperatures the distance between the two outmost layers expands in comparison with the bulk layers³⁹. The potential for aluminum used in this paper gives good description of the Al(111) relaxation, i.e., it gives the experimental value for surface relaxation $+0.9\%$ at $T = 90$ K^{20,39}. In this work the temperature dependence of surface relaxation was studied and results are also presented in Table I. It was found that this unusual outward expansion of the distance between the two top layers increases with temperature. This increase is $\sim 1\%$ along the superheating temperature region. The maximum of surface relaxation is $+3.3\%$ at the onset of melting.

B. Metastability

The fundamental questions of conditions and limits for the existence of any metastable state deserve further investigation. For metastable Al(111) it is important to consider a maximum of the superheating temperature as a function of aluminum properties. For fcc metal crystals the maximum of superheating should occur at the close packed non-melted (111) surfaces. MD simulation presented above shows that the mean-square vibrational amplitudes are isotropic at the transition from the superheated to liquid state (see Table I). Moreover, drops form everywhere, and

the liquid front rapidly propagates into the bulk. In the following estimate of the maximum superheating temperature small anisotropy of the solid-liquid interface free energy is not taken into account. Therefore, the spherical liquid nuclei are analyzed.

The kinetic theory of first order phase transitions provides a description of transformation from a metastable to stable phase¹⁷. This transition proceeds via fluctuation induced formation of the nuclei of the stable phase. If the radius r of the nucleus is smaller than some critical value r_c such nucleus disappears, if it is bigger the nucleus grows. The radius of the spherical liquid critical nucleus is

$$r_c = \frac{2\alpha}{L} \frac{T_m}{T - T_m}, \quad (2)$$

where α is the solid-liquid interface free energy and L is the latent heat of melting⁴⁰. It is possible to describe the growth of the nucleus by the kinetic Fokker-Planck equation for the distribution function $f(r, t)$

$$\frac{\partial f}{\partial t} = -\frac{\partial w}{\partial r}, \quad (3)$$

where w is the flux density. The phase transition corresponds to the stationary solution of Eq. (3), where $w = const$. Such solution is¹⁷

$$w = 2\sqrt{\frac{\alpha}{T}} B(r_c) f_0(r_c). \quad (4)$$

In this equation B is diffusion type coefficient and $f_0(r_c)$ is

$$f_0(r_c) = const \exp\left(\frac{-4\pi\alpha r_c^2}{3T}\right). \quad (5)$$

Equation (4) gives the rate for formation of a critical nucleus. The goal here is to calculate the maximum of superheating, i.e., the temperature at which melting occurs. Therefore, at this temperature $w \sim 1$. The coefficient $B(r_c)$ in Eq. (4), is given by¹⁷

$$B(r) = \frac{T}{8\pi\alpha(r - r_c)} \frac{dr}{dt}, \quad (6)$$

and can be calculated [for $r \rightarrow r_c$ as in Eq. (4)] by considering a particular metastable state.

For a transition from the superheated to liquid state it is necessary to consider the diffusive transport of heat at the liquid-solid interface^{18,19}. It is convenient to define the dimensionless field

$$u = \frac{C_p}{L}(T_\infty - T), \quad (7)$$

where T_∞ is the temperature of the solid infinitely far from the growing nucleus and C_p is the specific heat. Then the diffusion equation is

$$\frac{\partial u}{\partial t} = D \nabla^2 u, \quad (8)$$

where D is the thermal diffusion constant at $T \sim T_m$. One boundary condition is the heat conservation at the liquid-solid interface

$$v_n = -D \hat{n} \cdot \nabla u, \quad (9)$$

where \hat{n} is the unit normal directed outward from the nucleus and v_n is the normal growth velocity. There is also a requirement of local thermodynamic equilibrium that gives the dimensionless temperature u_l at the interface

$$u_l = \Delta - d_0 \mathcal{K}, \quad (10)$$

where

$$\Delta = \frac{C_p}{L}(T_\infty - T_m) \quad (11)$$

is proportional to superheating. In the second term in Eq. (10) (i.e., in the Gibbs-Thomson correction for the melting temperature at a curved surface) \mathcal{K} is the curvature and $d_0 = \alpha C_p T_m L^{-2}$. The solution for the growth rate of a spherical nucleus is¹⁹

$$\frac{dr}{dt} \Big|_{r \rightarrow r_c} \sim \frac{D}{r^2} (\Delta r_c - 2d_0). \quad (12)$$

Therefore, using Eqs. (5), (6), (12), and $T_\infty = T$, condition $w \sim 1$ for Eq. (4) gives

$$aT^{1/2}(T - T_m)^3 \exp\{-[b/T(T - T_m)^2]\} = 1, \quad (13)$$

where $a = DLC_p/16\pi\alpha^{5/2}T_m^2$ and $b = 16\pi\alpha^3T_m^2/3L^2$. Equation (13) was solved numerically using the experimental data for interface free energy α^4 , latent heat of melting L^4 , bulk melting temperature T_m^{23} , specific heat C_p^{23} , and diffusion constant D^{41} . The value ~ 23 K was obtained for the maximum of superheating. This value is smaller than the maximum superheating temperature of 180 K estimated in MD simulation for a model of the Al(111) surface. Part of this disagreement is the result of the approximate kinetic analysis and even possibly poor accuracy of some experimental data for Al. There is also a possibility that the value for the maximum of superheating found in MD simulations is in part the result of a limited time evolution. Although long runs of 10^6 time steps were performed in the superheating regime, much longer (nowadays not feasible) simulation times may give the maximum of the superheating temperature in accordance with the kinetic result. Using the kinetic analysis presented above, the same literature sources for α , L , T_m , C_p , and diffusion constant D from Ref.⁴², the value of ~ 47 K was obtained for the maximum superheating temperature of Pb. For aluminum a similar Fokker-Planck analysis was done using quantities deduced from the simulations. As in Ref.³¹, it was found that the bulk energy is slightly nonlinear function of temperature and that therefore it can be fitted by the second-order polynomial. Using this procedure³¹, the value of $C_p = 1120 \text{ J/(K kg)}$ was obtained, whereas the experimental value for the specific heat is 902 J/(K kg) [23]. For diffusion constant the value of $D = 0.3 \times 10^{-5} \text{ cm}^2/\text{s}$ was found (see also⁴³). This is much lower than the experimental value $3 \times 10^{-5} \text{ cm}^2/\text{s}^{41}$. When in Eq. (13) the quantities obtained in MD simulations for C_p , D , $L = 0.105 \text{ eV/atom}^{20}$, $T_m = 939 \text{ K}^{20}$, and $\alpha = 10 \text{ meV}\text{\AA}^{-2}$ ^{14,43} were used, then 48 K was calculated for the maximum superheating temperature of aluminum. It is important to point out that smaller values for the maximum superheating temperature were found in the experiments on the crystallites^{1,2,12}, whereas larger superheating was induced by a laser beam^{6–8,10}.

IV. SUMMARY AND CONCLUSIONS

The properties of a surface in the superheated state were studied using MD simulation and a reliable many-body interatomic potential. Superheated Al(111) was used as a model of superheated surfaces, such as ones obtained by a pulsed laser beam^{6–8,10}, or on the crystallites¹². A detailed analysis of the Al(111) surface from room temperature to 1500 K (i.e., well above the bulk melting point) was carried out. The results for lower temperatures are in a good agreement with available experimental observations and other MD simulations and electronic structure calculations for metal surfaces. It is possible to superheat the sample by ~ 180 K for typical longest simulation times used in classical MD (> 2.5 ns). In the superheating regime the Al(111) surface is remarkably well ordered, although single adatoms sometimes appear. The sample melts over the narrow temperature interval. Anomalous outward expansion between two top layers increases slowly with the temperature: from +0.9% at $T = 0$, up to +3.3% at the end of the superheating region. The mean-square vibrational amplitudes are isotropic for all temperatures and ~ 10 times larger at the end of the superheating region than below the bulk melting point. It was shown that kinetic theory based on the Fokker-Planck equation and analysis of heat conservation at the liquid-solid interface for aluminum gives the maximum superheating temperature of 23 K when experimentally determined parameters were used. The maximum superheating temperature of 48 K was obtained when parameters deduced from MD simulations were applied in the Fokker-Planck analysis. This analysis of kinetics and process of disordering observed in MD simulation shows that superheated Al(111) and bulk Al below the surface are an example of metastability at the solid-to-liquid transition. The kinetics of this transition is the same as in other better known examples of metastability¹⁷. Superheated surfaces of other metals should exhibit similar behavior.

ACKNOWLEDGMENTS

I would like to thank F. Ercolessi, B. Gumhalter, and E. Tosatti for discussions.

¹ L. Gråbek, J. Bohr, E. Johnson, A. Johansen, L. Sarholt-Kristensen, and H. H. Andersen, Phys. Rev. Lett. **64**, 934 (1990).

² J. Daeges, H. Gleiter, and J. H. Perepezko, Phys. Lett. A **119**, 79 (1986).

³ J. Q. Broughton, Phys. Rev. Lett. **67**, 2990 (1991).

⁴ J. F. van der Veen, B. Pluis, and A. W. Denier van der Gon, in *Chemistry and Physics of Solid Surfaces VII*, edited by R. Vanselow and R. F. Howe (Springer, Berlin, 1988), p. 455.

⁵ J. A. W. Denier van der Gon, R. J. Smith, J. M. Gay, D. J. O' Connor, and J. F. van der Veen, Surf. Sci. **227**, 143 (1990).

⁶ J. W. Herman and H. E. Elsayed-Ali, Phys. Rev. Lett. **69**, 1228 (1992).

⁷ E. A. Murphy, H. E. Elsayed-Ali, and J. W. Herman, Phys. Rev. B **48**, 4921 (1993).

⁸ J. W. Herman, H. E. Elsayed-Ali, and E. A. Murphy, Phys. Rev. Lett. **71**, 400 (1993).

⁹ J. W. Herman and H. E. Elsayed-Ali, Phys. Rev. Lett. **68**, 2952 (1992).

¹⁰ J. W. Herman and H. E. Elsayed-Ali, Phys. Rev. B **49**, 4886 (1994).

¹¹ H. Häkkinen and U. Landman, Phys. Rev. Lett. **71**, 1023 (1993).

¹² J. J. Metois and J. C. Heyraud, J. Phys. **50**, 3175 (1989).

¹³ P. Carnevali, F. Ercolessi, and E. Tosatti, Phys. Rev. B **36**, 6701 (1987).

¹⁴ F. D. Di Tolla, F. Ercolessi, and E. Tosatti, Phys. Rev. Lett. **74**, 3201 (1995).

¹⁵ H. Häkkinen and M. Manninen, Phys. Rev. B **46**, 1725 (1992).

¹⁶ G. Bilalbegović, F. Ercolessi, and E. Tosatti, Europhys. Lett. **17**, 333 (1992).

¹⁷ E. M. Lifshitz and L. P. Pitaevskii, *Physical Kinetics* (Pergamon, Oxford, 1981), Chap. XII.

¹⁸ J. S. Langer, in *Chance and Matter*, edited by J. Souletie, J. Vannimenu, and R. Stora (North-Holland, Amsterdam, 1987), Les Houches, Series XLVI, p. 629.

¹⁹ H. Muller-Krumbhaar and W. Kurz, in *Phase Transformations in Materials*, edited by P. Haasen (VCH-Verlag, Weinheim, 1991), p. 553.

²⁰ F. Ercolessi and J. B. Adams, Europhys. Lett. **26**, 583 (1994).

²¹ M. S. Daw and M. I. Baskes, Phys. Rev. B **29**, 6443 (1984).

²² A. M. Raphuthi, X. Q. Wang, F. Ercolessi, and J. B. Adams, Phys. Rev. B **52**, 5554 (1995).

²³ J. Emsley, *The Elements*, (Oxford University Press, Oxford, 1996), 3rd edition, and G. W. C. Kaye and T. H. Laby, *Tables of physical and chemical constants*, (Longman, London, 1993), 15th edition, as discussed in *WebElements*, <http://www.shef.ac.uk/~chem/web-elements/>, (University of Sheffield, Sheffield, 1996).

²⁴ J. R. Morris, C. Z. Wang, K. M. Ho, and C. T. Chan, Phys. Rev. B **49**, 3109 (1994).

²⁵ F. Ercolessi, O. Tomagnini, S. Iarlori, and E. Tosatti, in *Nanosources and Manipulation of Atoms under High Fields and Temperatures: Applications*, edited by Vu Thien Binh, N. Garcia, and K. Dransfeld (Kluwer, Dordrecht, 1993), NATO ASI Series E, Vol. 235, p. 185.

²⁶ R. C. Cammarata, Prog. Surf. Sci. **46**, 1 (1994).

²⁷ J. Q. Broughton and G. H. Gilmer, J. Chem. Phys. **79**, 5105 (1983).

²⁸ F. Ercolessi, S. Iarlori, O. Tomagnini, E. Tosatti, and X. J. Chen, Surf. Sci. **251/252**, 645 (1991).

²⁹ G. Bilalbegović and E. Tosatti, Phys. Rev. B **48**, 11240 (1993).

³⁰ G. Bilalbegović, Phys. Rev. B **53**, 1616 (1996).

³¹ B. D. Todd and R. M. Lynden-Bell, Surf. Sci. **281**, 191 (1993).

³² R. J. Needs and M. J. Godfrey, Phys. Rev. B **42**, 10933 (1990).

³³ P. J. Feibelman, Phys. Rev. B **50**, 1908 (1994).

³⁴ M. Schmid, W. Hofer, P. Varga, P. Stoltze, K. W. Jacobsen, and J. K. Nørskov, Phys. Rev. B **51**, 10937 (1995).

³⁵ S. M. Thompson, K. E. Gubbins, J. P. R. B Walton, R. A. R. Chantry, and J. S. Rowlinson, J. Chem. Phys. **81**, 530 (1984); M. P. Allen and D. J. Tildesley, *Computer Simulation of Liquids* (Clarendon, Oxford, 1987).

³⁶ L. Yang, T. S. Rahman, and M. S. Daw, Phys. Rev. B **44**, 13725 (1991).

³⁷ Y. Beaudet, L. J. Lewis, and M. Persson, Phys. Rev. B **50**, 12084 (1994).

³⁸ Q. T. Jiang, P. Fenter, and T. Gustafsson, Phys. Rev. B **44**, 5773 (1991); B. M. Ocko, D. Gibbs, K. G. Huang, D. M. Zehner, and S. G. J. Mochrie, *ibid.* **44**, 6429 (1991).

³⁹ H. B. Nielsen and D. L. Adams, J. Phys. C **15**, 615 (1982).

⁴⁰ L. D. Landau and E. M. Lifshitz, *Statistical Physics* (Pergamon, Oxford, 1980), Sec. 162.

⁴¹ W. Ludwig, *Diploma work*, University of Münster, Münster, 1969, as discussed in W. Schommers, C. Mayer, H. Göbel, and P. von Blanckenhagen, J. Vac. Sci. Technol. A **13**, 1413 (1995).

⁴² N. H. Nachtrieb, Ber. Bunsenges. **80**, 678 (1976), as discussed in J. W. M. Frenken, B. J. Hinch, J. P. Toennies, and Ch. Wöll, Phys. Rev. B **41**, 938 (1990).

⁴³ F. D. Di Tolla, Ph.D. thesis, SISSA Trieste, 1996.

TABLE I. Mean-square vibrational amplitudes for the Al(111) surface (in units of \AA^2): u_x^2 (along the $[1\bar{1}0]$ direction), u_y^2 (along the $[11\bar{2}]$ direction) and u_z^2 (along the vertical axis). The surface relaxation d_{12} between the two top layers is also shown (in %).

Temperature	u_x^2	u_y^2	u_z^2	d_{12}
300 K	0.014	0.022	0.018	+1.1
900 K	0.074	0.064	0.075	+2.2
1050 K	0.118	0.119	0.101	+2.4
1120 K	0.839	0.708	0.731	+3.3

FIG. 1. Particle trajectories showing the superheated surface after 10^6 MD steps of time evolution at 1050 K (i.e., 110 K above the bulk melting temperature): (a) top view, (b) side view with an adatom above the surface. Trajectory plots refer to a time span of ~ 3 ps and include only moving atoms.

FIG. 2. The caloric curve. The vertical line represents the calculated bulk melting temperature.

FIG. 3. Surface stress as a function of temperature. The dashed vertical lines enclose the superheating region.

This figure "Fig1.gif" is available in "gif" format from:

<http://arXiv.org/ps/cond-mat/9704045v1>

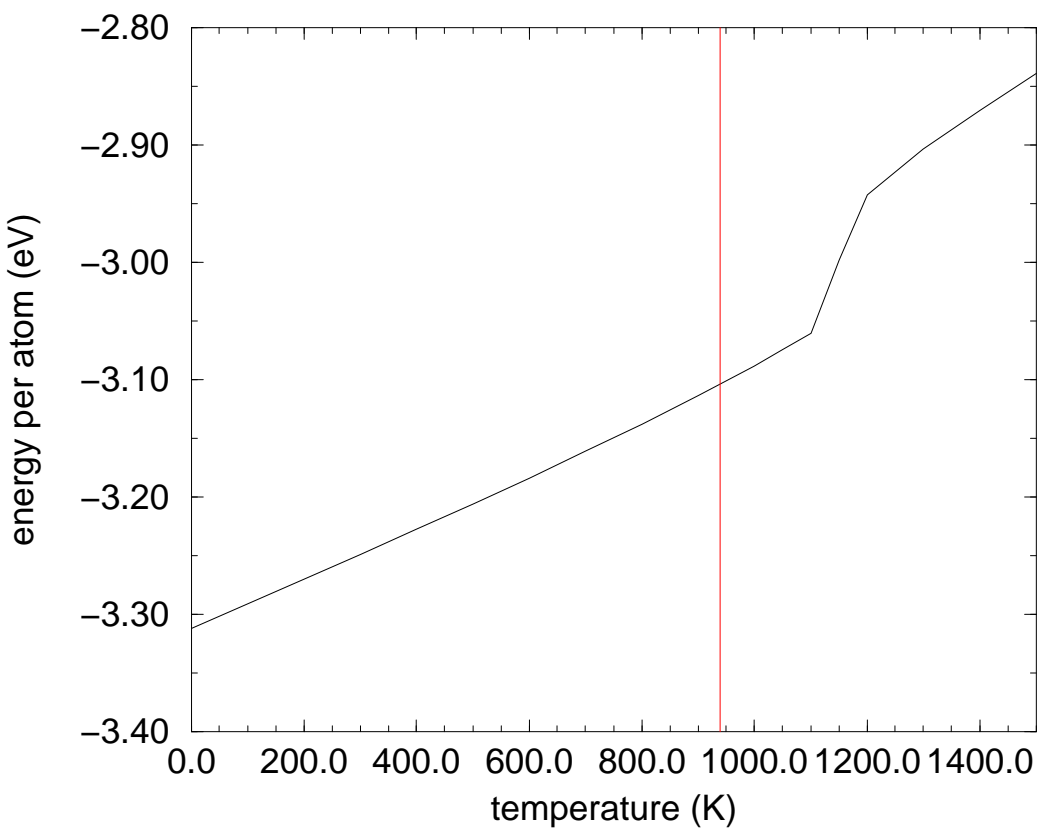


Fig. 2
G. Bilalbegovic

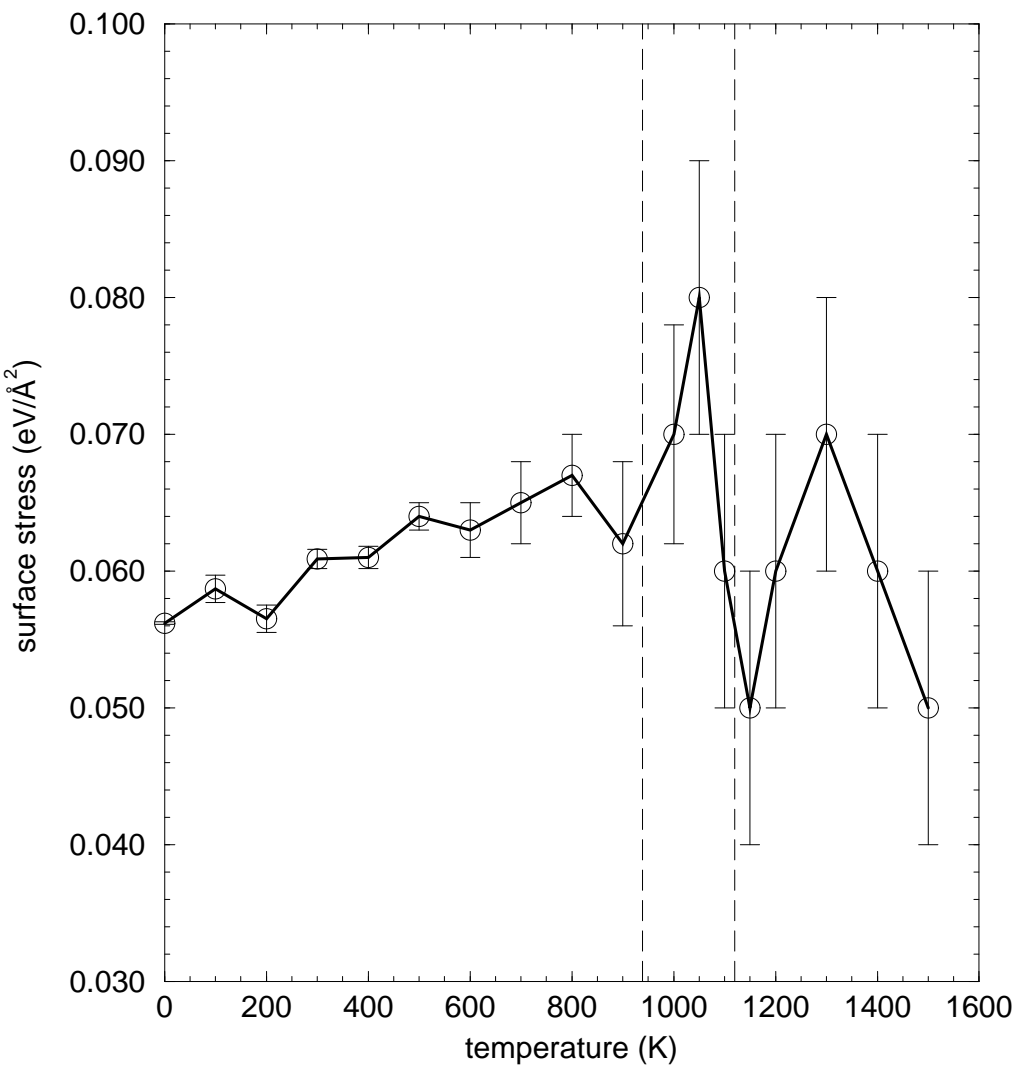


Fig. 3
G. Bilalbegovic